Glycerol-3-Phosphate Acyltransferase 1 Deficiency in *ob/ob* Mice Diminishes Hepatic Steatosis but Does Not Protect Against Insulin Resistance or Obesity

Angela A. Wendel,[1] Lei O. Li,[1] Yue Li,[1] Gary W. Cline,[2] Gerald I. Shulman,[2,3] and Rosalind A. Coleman[1]

OBJECTIVE—Hepatic steatosis is strongly associated with insulin resistance, but a causal role has not been established. In *ob/ob* mice, sterol regulatory element binding protein 1 (SREBP1) mediates the induction of steatosis by upregulating target genes, including glycerol-3-phosphate acyltransferase-1 (*Gpat1*), which catalyzes the first and committed step in the pathway of glycerolipid synthesis. We asked whether *ob/ob* mice lacking *Gpat1* would have reduced hepatic steatosis and improved insulin sensitivity.

RESEARCH DESIGN AND METHODS—Hepatic lipids, insulin sensitivity, and hepatic insulin signaling were compared in lean ($Lep^{+/?}$), lean-$Gpat1^{-/-}$, *ob/ob* ($Lep^{ob/ob}$), and *ob/ob*-$Gpat1^{-/-}$ mice.

RESULTS—Compared with *ob/ob* mice, the lack of Gpat1 in *ob/ob* mice reduced hepatic triacylglycerol (TAG) and diacylglycerol (DAG) content 59 and 74%, respectively, but increased acyl-CoA levels. Despite the reduction in hepatic lipids, fasting glucose and insulin concentrations did not improve, and insulin tolerance remained impaired. In both *ob/ob* and *ob/ob*-$Gpat1^{-/-}$ mice, insulin resistance was accompanied by elevated hepatic protein kinase C-ε activation and blunted insulin-stimulated Akt activation.

CONCLUSIONS—These results suggest that decreasing hepatic steatosis alone does not improve insulin resistance, and that factors other than increased hepatic DAG and TAG contribute to hepatic insulin resistance in this genetically obese model. They also show that the SREBP1-mediated induction of hepatic steatosis in *ob/ob* mice requires *Gpat1*.
***Diabetes* 59:1321–1329, 2010**

Ob/ob mice are leptin deficient and become hyperphagic, obese, and insulin resistant (1). Severe hepatic steatosis in *ob/ob* mice is secondary to hepatic upregulation of sterol regulatory element binding protein 1 (SREBP1) and its target genes that increase lipogenesis and triacylglycerol (TAG) synthesis (2). Among these target genes is *Gpat1*, which encodes glycerol-3-phosphate acyltransferase-1, the mitochondrial enzyme that catalyzes the reaction glycerol-3-phosphate + long-chain acyl-CoA → lysophosphatidic acid, the committed step in the pathway of de novo glycerolipid synthesis (3). Four isoforms of glycerol-3-phosphate acyltransferase (GPAT), each encoded by a separate gene, are able to initiate the glycerolipid synthesis (4), but only *Gpat1* is regulated by SREBP1 (5). GPAT1 activity and mRNA are highest in tissues with a high capacity for TAG synthesis; in liver, the GPAT1 isoform accounts for 30–50% of total GPAT activity. Hepatic GPAT1 activity and mRNA abundance are increased by insulin via activation of liver X receptor (LXR) and SREBP1c during conditions that promote TAG synthesis (5). Conversely, glucagon, fasting, and streptozotocin-induced diabetes decrease liver GPAT1 mRNA and activity (6).

Elevated hepatic TAG content in humans has been linked to insulin resistance (7–9). In rats increasing hepatic TAG content by adenovirus-mediated overexpression of GPAT1 induced hepatic and peripheral insulin resistance within 5–7 days (10). Conversely, $Gpat1^{-/-}$ mice fed a high-fat safflower oil diet for 3 weeks were protected from hepatic steatosis and insulin resistance (11).

Although studies strongly suggest that reducing hepatic steatosis improves hepatic insulin sensitivity (11–14), it is unlikely that the accumulation of hepatic TAG itself, rather than another glycerolipid metabolite such as diacylglycerol (DAG), plays a causal role in impaired hepatic insulin signaling (15). Furthermore, the role of GPAT1 in hepatic steatosis has been questioned because both $Gpat1^{-/-}$ mice fed a high-fat/high-sucrose diet for 4 months (16) and an independently derived $Gpat1^{-/-}$ mouse strain fed a high-fat diet for 3 months (17) developed hepatic steatosis and became insulin resistant, although both developed in the context of obesity.

Because the insulin-sensitizing effects that occur when deleted *Gpat1* reduces hepatic steatosis appear to be highly sensitive to diet composition and duration, we investigated *ob/ob* mice to determine whether the absence of *Gpat1* would improve hepatic steatosis and insulin resistance associated with genetic-induced obesity. Hepatic steatosis in *ob/ob* mice is associated with a 2.3-fold increase in GPAT1 activity and a 5.5-fold increase in *Gpat1* mRNA (18). Because a 5-day 90% adenovirus-mediated knockdown of hepatic *Gpat1* in *ob/ob* mice resulted in a 42% reduction in hepatic TAG and a 30% decrease in plasma glucose (19), we hypothesized that a total lack of *Gpat1* in *ob/ob* mice would prevent both hepatic steatosis and insulin resistance.

From the [1]Department of Nutrition, University of North Carolina, Chapel Hill, North Carolina; the [2]Departments of Internal Medicine and Cellular & Molecular Physiology, Yale University School of Medicine, New Haven, Connecticut; and the [3]Howard Hughes Medical Institute, Yale University School of Medicine, New Haven, Connecticut.

Corresponding author: Rosalind Coleman, rcoleman@unc.edu.

Received 16 September 2009 and accepted 22 February 2010. Published ahead of print at http://diabetes.diabetesjournals.org on 3 March 2010. DOI: 10.2337/db09-1380.

RESEARCH DESIGN AND METHODS

Mice. Animal protocols were approved by the University of North Carolina at Chapel Hill Institutional Animal Care and Use Committee. Mice were housed in a pathogen-free barrier facility on a 12-h light/dark cycle with free access to water and food (Prolab 5P76 Isopro 3000; 5.4% fat by weight). To generate *Gpat1*$^{-/-}$ mice on an obese background, *Gpat1*$^{+/-}$ mice (20), which have been backcrossed to C57BL/6J mice seven times, were crossed with *Lep*$^{+/ob}$ mice (B6.V-Lep^{ob}/J; The Jackson Laboratory, Bar Harbor, ME). After crossing the double heterozygotes, *Lep*$^{+/ob}$-*Gpat1*$^{+/+}$ or *Lep*$^{+/ob}$-*Gpat1*$^{-/-}$ mice were then intercrossed to generate *Lep*$^{ob/ob}$-*Gpat1*$^{+/+}$ or *Lep*$^{ob/ob}$-*Gpat1*$^{-/-}$ mice and their respective lean (*Lep*$^{+/?}$) littermates. Male mice were used in all experiments. At 16 weeks, total lean and fat mass was measured using an EchoMRI-100 QNMR system (Echo Medical Systems, LLC, Houston, TX). Fasted (12 h) 16-week-old mice were killed by cervical dislocation, and trunk blood was collected. Clotted blood was centrifuged at 1,500*g* for 20 min and sera were stored at −80°C until analyzed. Tissues were quickly harvested, weighed, snap-frozen with liquid nitrogen, and stored at −80°C until analyzed. Liver sections were fixed with 4% paraformaldehyde, paraffin-embedded, sectioned (0.5 μm), and stained with hematoxylin-eosin.

Serum chemistries and lipids. Serum nonesterified fatty acids and total cholesterol (Wako Diagnostics, Richmond, VA), β-hydroxybutyrate (Stanbio, Boerne, TX), and triacylglycerol and glycerol (free glycerol and triglyceride reagents; Sigma-Aldrich, St. Louis, MO) were determined by enzymatic, colorimetric assays. Insulin was determined by enzyme-linked immunosorbent assay (Rat/Mouse Insulin ELISA; Millipore, Billerica, MA).

GPAT activity. Liver tissue was homogenized in Medium I (250 mmol/l sucrose, 10 mmol/l Tris, pH 7.4, 1 mmol/l EDTA, 1 mmol/l dithiothreitol) with 10 up-and-down strokes with a Teflon-glass motor-driven homogenizer. Homogenates were centrifuged at 100,000*g* for 1 h to obtain total membrane fractions. Membrane pellets were rehomogenized in Medium I. GPAT specific activity was assayed at room temperature in a 200 μl reaction mixture containing 75 mmol/l Tris-HCl, pH 7.5, 4 mmol/l $MgCl_2$, 1 mg/ml BSA (essentially fatty acid–free), 1 mmol/l dithiothreitol, 8 mmol/l NaF, 800 μmol/l [^{3}H]glycerol 3-phosphate, and 80 μmol/l palmitoyl-CoA (20). The reaction was initiated by adding 10–30 μg of membrane protein after incubating the membrane protein on ice for 15 min in the presence or absence of 2 mmol/l *N*-ethylmaleimide (NEM), which inactivates GPAT isoforms 2, 3, and 4. NEM-resistant activity (GPAT1) was calculated by subtracting NEM-sensitive activity from total activity.

Quantitative real-time RT-PCR. RNA was extracted from liver using Trizol (Invitrogen, Carlsbad, CA) and reverse-transcribed with the High-Capacity cDNA Archive kit (Applied Biosystems, Foster City, CA). cDNA was amplified by real-time PCR in a total reaction volume of 25 μl using Absolute QPCR Sybr Green Fluorescein Mix (ThermoScientific, Waltham, MA). Primer sets are identified in supplementary Table 1, available in an online appendix at http://diabetes.diabetesjournals.org/content/early/2010/03/02/db09-1380/suppl/DC1. Target gene expression was normalized to endogenous 18S rRNA and expressed as $2^{-\Delta\Delta ct}$ relative to the lean-*Gpat1*$^{+/+}$ group (21).

Tissue lipid metabolites. Tissues were homogenized in 10× (wt/vol) cold lysis buffer (20 mmol/l Tris base, 50 mmol/l NaCl, 250 mmol/l sucrose, 50 mmol/l NaF, 5 mmol/l $Na_4P_2O_7{\cdot}10\ H_2O$, 1% Triton X-100, and protease inhibitors). Lipids were extracted (22), dried under N_2 gas, and solubilized in 3:1:1 (vol/vol/vol) tert-butanol, methanol, and Triton X-100 (23). Tissue lipid extracts were analyzed for TAG by an enzymatic assay (Triglyceride and Free-Glycerol reagents; Sigma-Aldrich). Data are expressed as equivalent triolein concentrations.

DAG and acyl-CoAs were extracted and measured by liquid chromatography–tandem mass spectrometry (11). For ceramides, ~50 mg of tissue was homogenized with 1 ml ice-cold methanol. Chloroform (2 ml) and an internal standard (5 nmol C17:0 ceramide; Avanti Polar Lipids, Inc., Alabaster, AL) were added, the sample was mixed for 15 min, and water (0.6 ml) was added. After centrifugation at 4°C, the organic layer was collected, dried overnight in a vacuum oven, and reconstituted with chloroform.

Lipid metabolites were subjected to liquid chromatography–tandem mass spectrometry analysis. A turbo ion spray source was interfaced with an API 3000 tandem mass spectrometer (Applied Biosystems) in conjunction with two Perkin Elmer 200 Series micropumps and a 200 Series autosampler (Perkin Elmer, Norwalk, CT). Total acyl-CoA, ceramide, and DAG content were expressed as the sum of individual species.

Insulin tolerance tests. At 15 weeks of age, after an overnight (12 h) fast, mice were injected intraperitoneally with insulin (Humulin: R; Eli Lilly, Indianapolis, IN) at either 0.5 units/kg body wt (lean mice) or 1.5 units/kg body wt (*ob/ob* mice). Glucose in tail vein blood was measured immediately before injection (time 0) and at 15, 30, 60, 90, and 120 min after injection (One Touch Ultra glucometer; Lifescan, Milpitas, CA). Areas of the curves were calculated as the net area contained between individual baselines (set by the glucose value at time 0) and curves using the trapezoidal rule (24).

Western blot analysis. Protein kinase C-ε (PKCε) membrane translocation was determined by immunoblotting cytosol and membrane protein extracts (40 μg) with rabbit anti-PKCε (1:100; Santa Cruz Biotechnology, Santa Cruz, CA) (25,26). Translocation for each sample was determined as the ratio of the density of PKCε of the membrane fraction over the density of PKCε of the cytosolic fraction.

To evaluate insulin signaling, after an overnight (12 h) fast, insulin (2 units/kg body wt) or PBS was administered intraperitoneally to 6- or 16-week-old mice. After 10 min, mice were killed by cervical dislocation, and livers were excised and snap-frozen in liquid nitrogen. Tissues were homogenized in lysis buffer (20 mmol/l Tris, 150 mmol/l NaCl, 1 mmol/l EDTA, 1 mmol/l EGTA, 50 mmol/l NaF, 2.5 mmol/l $Na_4P_2O_7{\cdot}10\ H_2O$, 1% Triton X-100, and Complete Mini Protease Inhibitor Cocktail; Roche Diagnostics, Indianapolis, IN) and centrifuged at 15,000*g* for 15 min. Protein (40 μg) was resolved on 10% polyacrylamide gels, transferred to nitrocellulose membranes, probed for phosphorylated Akt (P-Akt; Thr308; 1:1,000), stripped, and reprobed for total Akt and α-tubulin (Cell Signaling Technology, Danvers, MA). Mature SREBP1 (Novus Biologicals, LLC, Littleton, CO) and phosphoenolpyruvate carboxykinase (Abcam Inc., Cambridge, MA) protein expression was determined from livers of mice fasted overnight (12 h) using the same method.

Statistical analyses. Data are expressed as least square means (LSM) ± SEM. The main and interaction effects of the *ob* phenotype (lean and *ob/ob*) and *Gpat1* genotype (*Gpat1*$^{+/+}$ and *Gpat1*$^{-/-}$) were analyzed by two-way ANOVA using a complete model in the general linear model (GLM) procedure of the SAS (Version 9.2; SAS Institute, Inc., Cary, NC). Body weights over time and insulin tolerance test curves were analyzed as repeated measures. Comparisons of basal versus insulin-stimulated Akt expression within group were analyzed by Student *t* test. Differences of $P < 0.05$ were considered significant.

RESULTS

The absence of *Gpat1* diminished hepatic steatosis in *ob/ob* mice. Hepatic steatosis in *ob/ob* mice is mediated by SREBP1c, which increases the expression of lipogenic genes (27), including *Gpat1* (5). To determine the contribution of *Gpat1* to the development of hepatic steatosis in *ob/ob* mice, we intercrossed *ob/ob* and *Gpat1*$^{-/-}$ mice. Compared with lean littermates, total hepatic GPAT specific activity in *ob/ob* mice was 33% higher, and both GPAT1 activity (NEM-resistant GPAT; Fig. 1*A*) and mRNA expression (Fig. 1*B*) were 2.2-fold higher. In *ob/ob* mice lacking *Gpat1* (*ob/ob*-*Gpat1*$^{-/-}$), total GPAT activity was reduced to levels observed in lean mice, and GPAT1 activity was diminished. The absence of *Gpat1* induced a 28% increase in NEM-sensitive GPAT activity (GPAT2, GPAT3, and GPAT4) in *ob/ob* mice (Fig. 1*A*). This increase in NEM-sensitive GPAT activity was likely due to increases in both *Gpat-3* and *-4* expression, although only the increase of *Gpat3* mRNA expression in *ob/ob* mice was significant (supplementary Fig. 1*B* and *C*). Collectively, the data suggest that elevated GPAT1 activity is required for the increase in TAG accumulation in *ob/ob* liver (28). Furthermore, the slight increase in activity and message of GPAT3 and GPAT4 did not compensate for the decrease in total GPAT activity in *Gpat1*$^{-/-}$ mice.

As previously reported (28), *ob/ob* mice developed grossly steatotic livers with macrosteatosis and microsteatosis that weighed four times more than livers from lean littermates (Table 1) and accumulated nearly five times as much TAG (Fig. 2*A* and *B*). In *ob/ob*-*Gpat1*$^{-/-}$ mice, the lack of *Gpat1* reduced liver weight by 28% and hepatic TAG content by 59%, evidenced by the absence of large lipid droplets. In *ob/ob* livers, the lipogenic genes fatty acid synthase (*Fasn*) and stearoyl-CoA desaturase 1 (*Scd1*) were increased 4- and 6.4-fold, respectively. However, neither *Fasn* and *Scd1* nor transcription factors that regulate lipogenesis, SREBP1 (*Srebf1*) and ChREBP (*Mlxipl*), were affected by the lack of *Gpat1* (supplemen-

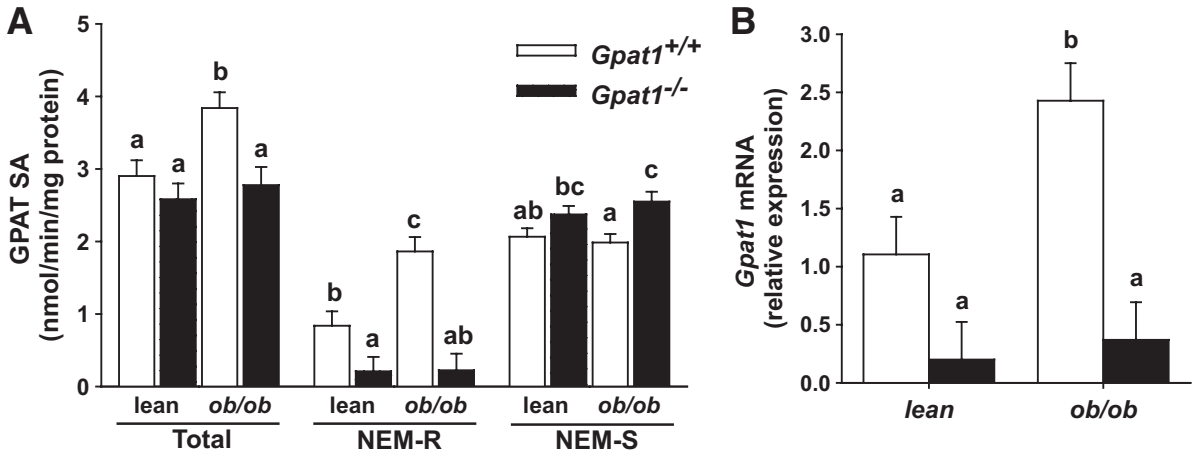

FIG. 1. ***A*****: Total, NEM-resistant (NEM-R), and NEM-sensitive (NEM-S) GPAT specific activities. Liver total particulate fractions (n = 3–4) were assayed for GPAT activity in the presence or absence of 2 mmol/l NEM as described in the "RESEARCH DESIGN AND METHODS" section.** ***B*****: Hepatic gene expression of *Gpat1* was determined by quantitative RT-PCR and expressed as $2^{-\Delta\Delta ct}$ relative to the endogenous control 18S rRNA and the lean-*Gpat1*$^{+/+}$ group (n = 4). Lean (*Lep*$^{+/?}$) and *ob/ob* (*Lep*$^{ob/ob}$). Data are LSM ± SE. Significant differences ($P < 0.05$) are denoted by different letters. SA, specific activity.**

tary Fig. 2*A*). Similarly, protein expression of the mature form of SREBP1 was not affected by the absence of *Gpat1* (supplementary Fig. 2*B*). The expression of genes related to β-oxidation was not altered (supplementary Fig. 2*C*). Combined, these data suggest that *Gpat1* appeared to be a major SREBP1 target gene causing hepatic steatosis in *ob/ob* mice.

Lack of *Gpat* did not protect *ob/ob* mice from insulin resistance. Because an acute knockdown of *Gpat1* decreases plasma glucose in *ob/ob* mice (19), we then asked whether the elevated fasting glucose and insulin levels or the insulin resistance that is normally observed in *ob/ob* mice might be improved by a sustained decrease in hepatic TAG. At 16 weeks of age, compared with lean mice, *ob/ob* mice had 1.7- and 16.2-fold higher serum fasting glucose and insulin concentrations, respectively (Fig. 2*C* and *D*). The absence of *Gpat1* did not reduce glucose or insulin; on the contrary, both were higher in *ob/ob-Gpat1*$^{-/-}$ mice than in *ob/ob* mice. The elevated glucose levels in the absence of *Gpat1* may be explained partly by an increase in hepatic glucose-6-phosphate (*G6pc*) mRNA expression, a key enzyme in gluconeogenesis. However, mRNA and protein expression of phosphoenolpyruvate carboxykinase was not altered (supplementary Fig. 2*D* and *E*). In addition to not improving fasting glucose and insulin, the absence of *Gpat1* did not affect insulin sensitivity in either lean or *ob/ob* mice (Fig. 2*E* and *F*).

Because hepatic steatosis and insulin resistance are progressive disorders that likely affected multiple tissues in 16-week-old *ob/ob* mice, we examined younger mice to determine whether they might be more insulin sensitive. At 6 weeks, livers from *ob/ob* mice were already steatotic and contained 1.7-fold more hepatic TAG than livers from lean mice (supplementary Fig. 3*A*). The absence of *Gpat1* diminished hepatic TAG by 68 and 66% in young lean and *ob/ob* mice, respectively, and effectively normalized the content of hepatic TAG. Despite the normal hepatic TAG content and lowered fasting glucose concentrations in young *ob/ob* mice that lacked *Gpat1* (supplementary Fig. 3*B*), serum insulin remained elevated (supplementary Fig. 3*C*) and insulin sensitivity remained impaired (supplementary Fig. 3*D* and *E*). These data demonstrate that early-stage hyperinsulinemia and whole-body insulin resistance were not improved despite a normal content of hepatic TAG.

TABLE 1
Physiologic parameters and fasting serum analytes

	Lean (*Lep*$^{+/?}$)		*ob/ob* (*Lep*$^{ob/ob}$)		Factors (P value)		
	Gpat1$^{+/+}$	*Gpat1*$^{-/-}$	*Gpat1*$^{+/+}$	*Gpat1*$^{-/-}$	Pheno	*Gpat1*	Int
Physiologic parameters							
Final body wt (g)	28.8 ± 1.0^{a}	28.1 ± 0.9^{a}	57.2 ± 1.0^{b}	55.0 ± 0.9^{b}	<0.001	0.133	0.407
Lean mass (% body wt)	86.3 ± 0.9^{a}	86.3 ± 1.3^{a}	44.5 ± 0.9^{b}	41.9 ± 1.4^{b}	<0.001	0.473	0.090
Fat mass (% body wt)	13.0 ± 0.9^{a}	11.8 ± 1.3^{a}	54.9 ± 0.9^{b}	57.8 ± 1.4^{b}	<0.001	0.274	0.257
Liver weight (g)	1.04 ± 0.14^{a}	1.09 ± 0.17^{a}	3.90 ± 0.14^{c}	2.67 ± 0.16^{b}	<0.001	<0.001	<0.001
Serum analytes							
Nonesterified fatty acids (mmol/l)	1.03 ± 0.09	0.97 ± 0.09	1.17 ± 0.09	1.19 ± 0.1	0.056	0.826	0.672
Triacylglycerol (mmol/l)	1.04 ± 0.14^{ab}	0.81 ± 0.16^{a}	1.42 ± 0.14^{b}	1.43 ± 0.16^{b}	0.004	0.464	0.448
Glycerol (mmol/l)	0.46 ± 0.06^{ab}	0.32 ± 0.07^{a}	0.56 ± 0.06^{b}	0.54 ± 0.07^{b}	0.019	0.215	0.378
Total cholesterol (mmol/l)	3.11 ± 0.39^{a}	2.96 ± 0.39^{a}	6.86 ± 0.39^{b}	5.81 ± 0.39^{b}	<0.001	0.129	0.254
β-hydroxybutyrate (mmol/l)	0.69 ± 0.08^{bc}	0.83 ± 0.07^{c}	0.44 ± 0.07^{a}	0.52 ± 0.08^{ab}	0.001	0.141	0.710

Final body weights (n = 12–16) and fat and lean masses (n = 6–13) were measured at 16 weeks. Serum analytes (n = 4–9) were measured from sera of mice fasted for 12 h. Values represent LSM ± SE with significant differences ($P < 0.05$) within rows denoted by different letters. Factors include the main effects of phenotype (Pheno; lean or *ob/ob*) and *Gpat1* and their interaction (Int).

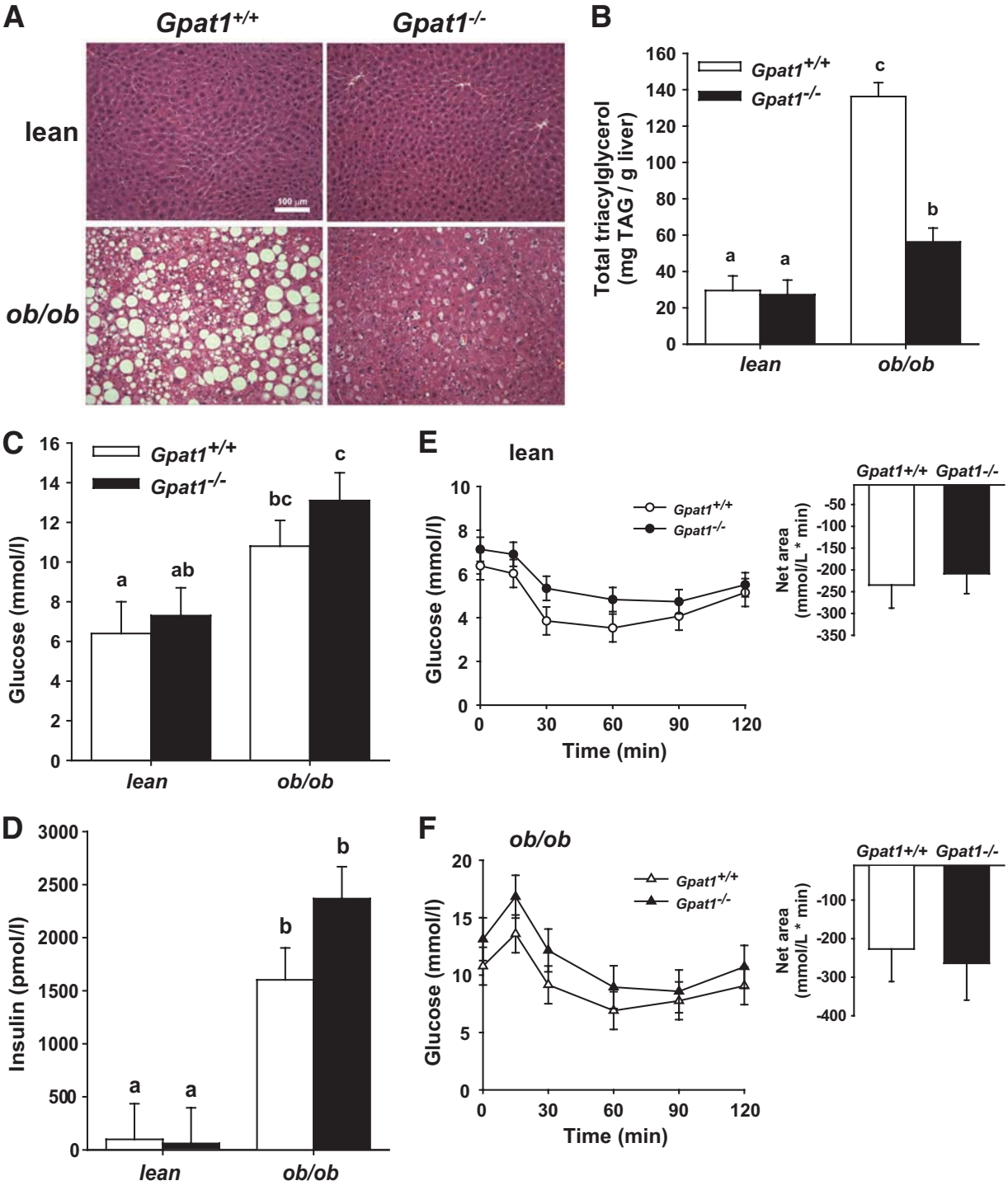

FIG. 2. Obesity-induced hepatic steatosis, but not insulin resistance, was diminished in *Gpat1*$^{-/-}$ mice. *A*: Representative liver sections stained with hematoxylin-eosin from 16-week-old male mice. Images are at ×100 magnification with 100 μm indicated by the white bar in upper left panel. *B*: Hepatic triacylglycerol content (n = 9–10). Fasting (*C*) glucose and (*D*) insulin. Insulin tolerance tests were conducted in 15-week-old male mice. Lean mice (*E*; n = 6–8) were given 0.5 units insulin/kg body wt by intraperitoneal injection, and *ob/ob* mice (*F*; n = 7–9) were administered 1.5 units insulin/kg body wt. Glucose was measured from tail vein blood at times indicated and net areas of the curves (insets) were calculated as described in the "RESEARCH DESIGN AND METHODS" section. Lean (*Lep*$^{+/?}$) and *ob/ob* (*Lep*$^{ob/ob}$). Data are expressed as LSM ± SE. Significant differences (P < 0.05) are denoted by different letters. (A high-quality digital representation of this figure is available in the online issue.)

Changes in hepatic lipids due to lack of *Gpat1*. Increases in the content of hepatic lipids such as DAG, acyl-CoA, and ceramide have been proposed to mediate hepatic insulin resistance (29,30). Compared with lean mice, total hepatic DAG in *ob/ob* liver was five times higher (Fig. 3*A*), and when *Gpat1* was absent, DAG content decreased to normal levels. The major DAG species reflected this pattern, with the largest differences apparent in C18:1-C18:1 and C18:1-C16:0 (Fig. 3*B*).

In *Gpat1*-null mice, liver acyl-CoA content is elevated twofold because acyl-CoAs are substrates for GPAT1 (11). Although phenotype (lean or *ob/ob*) did not have an effect on total hepatic acyl-CoA content, both lean and *ob/ob* livers deficient in *Gpat1* contained 3.3- and 5.3-fold more

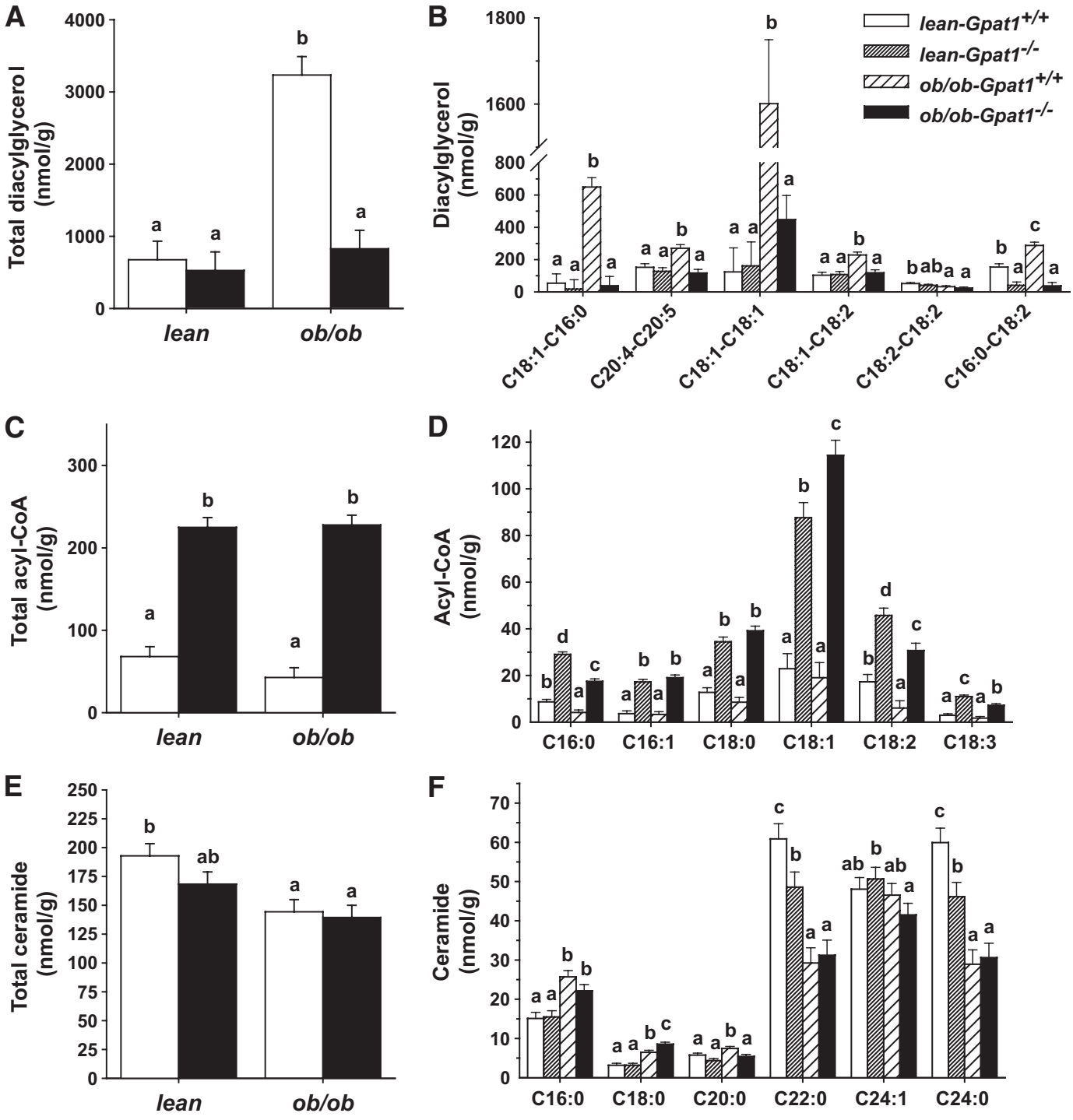

FIG. 3. Changes in hepatic lipids due to lack of *Gpat1*. *A* and *B*: Total hepatic diacylglycerol and species. *C* and *D*: Total acyl-CoA and species. *E* and *F*: Total ceramide and species ($n = 6$). Lipids were extracted from livers and measured as described in the "RESEARCH DESIGN AND METHODS" section. Lean (*Lep*$^{+/?}$) and *ob/ob* (*Lep*$^{ob/ob}$). Data are LSM ± SE. Significant differences ($P < 0.05$) are denoted by different letters.

total acyl-CoA than their *Gpat1*$^{+/+}$ counterparts, respectively (Fig. 3*C*). All the reported acyl-CoA species were increased, but the major one affected was 18:1-CoA, with 3.8- and 6.0-fold increases in lean- and *ob/ob-Gpat1*$^{-/-}$ mice, respectively (Fig. 3*D*).

In addition to TAG synthesis and β-oxidation, acyl-CoAs may also be directed toward the synthesis of ceramide, another purported modulator of insulin resistance (31). Compared with lean mice, the content of ceramide in livers from *ob/ob* mice was 25% lower (Fig. 3*E*), reflected primarily by fewer long-chain ceramides, C22:0 and C24:0 (Fig. 3*F*), even though C16:0 ceramide was higher. *Gpat1* deficiency did not significantly affect total ceramide content, but decreased C22:0 and C24:0 ceramides by ~52% in lean mice. Thus, total ceramide content was not associated with insulin resistance in this model.

Lack of *Gpat1* did not restore hepatic insulin signaling in *ob/ob* mice. Because both DAG and TAG decreased markedly in *Gpat1*-deficient liver, we examined the effect of *Gpat1* deficiency on insulin signaling. Hepatic steatosis

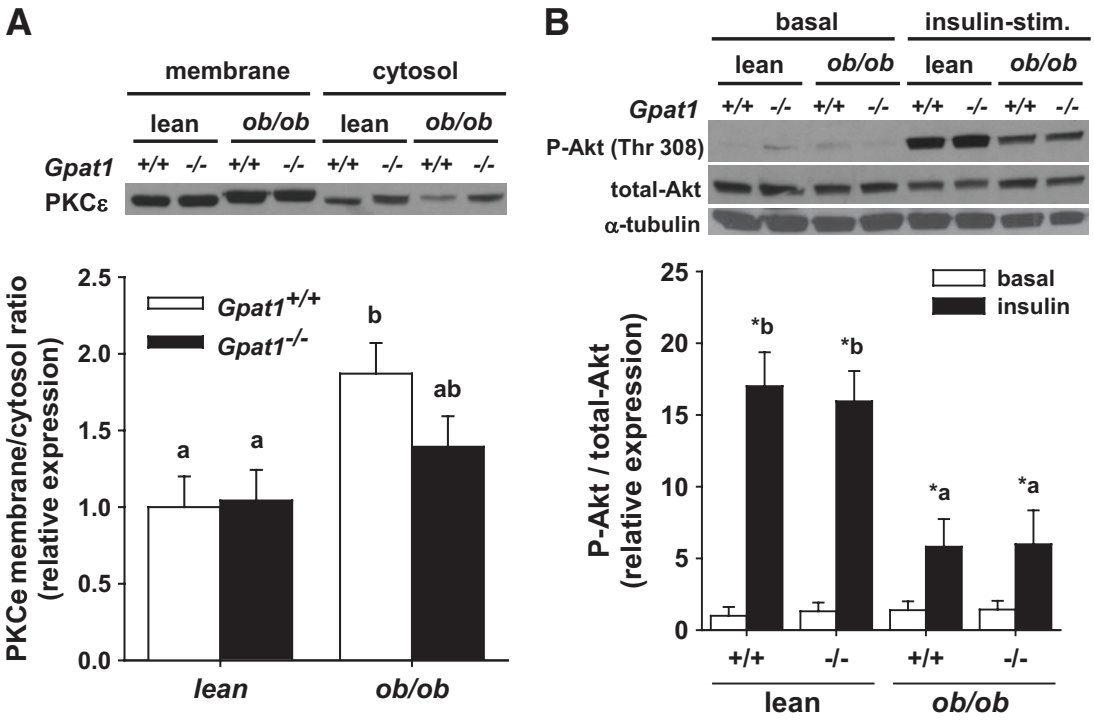

FIG. 4. Hepatic insulin signaling was not improved in *Gpat1*$^{-/-}$ mice. *A*: PKCε protein expression in cytosolic and membrane fractions of livers from 16-week-old mice was determined by Western blot analysis. Bars represent densities of the membrane to cytosolic ratio of PKCε expression relative to the lean-*Gpat1*$^{+/+}$ mice (n = 8). *B*: Basal and insulin-stimulated phosphorylated Akt expression. Mice were administered either 2.0 units insulin/kg body wt or PBS by intraperitoneal injection for 10 min. Bars represent densities of P-Akt/total Akt relative to the lean-*Gpat1*$^{+/+}$ mice (n = 4–5). Representative blots are shown. Lean (*Lep*$^{+/?}$) and *ob/ob* (*Lep*$^{ob/ob}$). Data are expressed as LSM ± SE. Significant differences (P < 0.05) among groups are denoted by different letters; * indicates a significant difference (P < 0.05) between basal and insulin-stimulated P-Akt/total Akt within group.

contributes to insulin resistance via increased DAG activation of PKCε and subsequent impairment of the insulin signaling pathway (11). To determine whether the improved hepatic lipid profile rescued hepatic insulin signaling, we examined activation of PKCε and Akt. In 16-week-old mice, concomitant with impaired insulin sensitivity, compared with lean mice, *ob/ob* mice had nearly twofold higher hepatic PKCε activation, marked by the increased ratio of membrane to cytosolic PKCε (Fig. 4*A*). Despite having a content of hepatic DAG similar to that of lean mice, PKCε activation was elevated in *ob/ob-Gpat1*$^{-/-}$ liver, although to a lesser extent than in *ob/ob* mice. At 6 weeks, no differences in hepatic PKC activation were detected among groups (supplementary Fig. 4*A*). Activated PKCε binds and inactivates the insulin receptor kinase, leading to impaired downstream insulin signaling, such as Akt activation (32). When either 16- or 6-week-old lean mice were stimulated with insulin, the amount of phosphorylated Akt in liver dramatically increased compared with basal expression (Fig. 4*B* and supplementary Fig. 4*B*). In *ob/ob* mice, however, the response to insulin was blunted by at least 65%, and this blunted response was not rescued when *Gpat1* was deficient. These data indicate that, although hepatic TAG and DAG content was considerably lower in *ob/ob-Gpat1*$^{-/-}$ mice, hepatic insulin signaling did not improve.

Lack of *Gpat1* did not reduce genetic obesity. Insulin resistance both in the liver and in peripheral tissues such as muscle and fat can contribute to whole-body insulin resistance. Although GPAT1 constitutes only 10% of total GPAT activity in adipose tissue, adipose GPAT1 specific activity is high (5), and female *Gpat1*$^{-/-}$ mice have reduced body and gonadal adipose depot weights (20). We determined whether the absence of *Gpat1* would reduce obesity in *ob/ob* mice. At 16 weeks, *ob/ob* mice weighed twice as much as their lean littermates (Fig. 5*A*; Table 1). However, the absence of *Gpat1* in lean or *ob/ob* mice did alter body weights over time or final body weights in either male (Fig. 5*A*; Table 1) or female (data not shown) mice. Compared with lean mice, gonadal, retroperitoneal, and inguinal white adipose and subscapular brown adipose tissue depots weighed dramatically more in the *ob/ob* mice, and were unaffected by the absence of *Gpat1* (Fig. 5*B*). Quantitative nuclear magnetic resonance analysis confirmed that the *Gpat1* deficiency did not have an effect on total lean or fat mass as a percentage of body weight (Table 1).

Lack of *Gpat1* did not improve muscle lipids. Obesity-mediated increases in muscle TAG content correlate strongly with whole-body insulin resistance (29). Even though GPAT1 specific activity is very low in muscle (5), we examined lipids in muscle to determine whether changes in muscular lipid could affect whole-body insulin resistance. In gastrocnemius muscle, the content of TAG and DAG in *ob/ob* mice was 4- and 2.3-fold higher, respectively (supplementary Fig. 5*A* and *B*). The absence of *Gpat1* in lean or *ob/ob* mice had no effect on muscle TAG or DAG content or on the DAG species present (supplementary Fig. 5*C*). Muscle acyl-CoA and ceramide content and molecular species in *ob/ob* mice were also unaffected by the absence of *Gpat1* (supplementary Fig. 5*D–G*).

The absence of *Gpat1* did not alter serum lipids. Corresponding with the development of obesity, serum cholesterol and TAG were elevated in *ob/ob* mice (33), whereas in *Gpat1*$^{-/-}$ mice, serum cholesterol is normal and serum TAG was reduced (11). The absence of *Gpat1*,

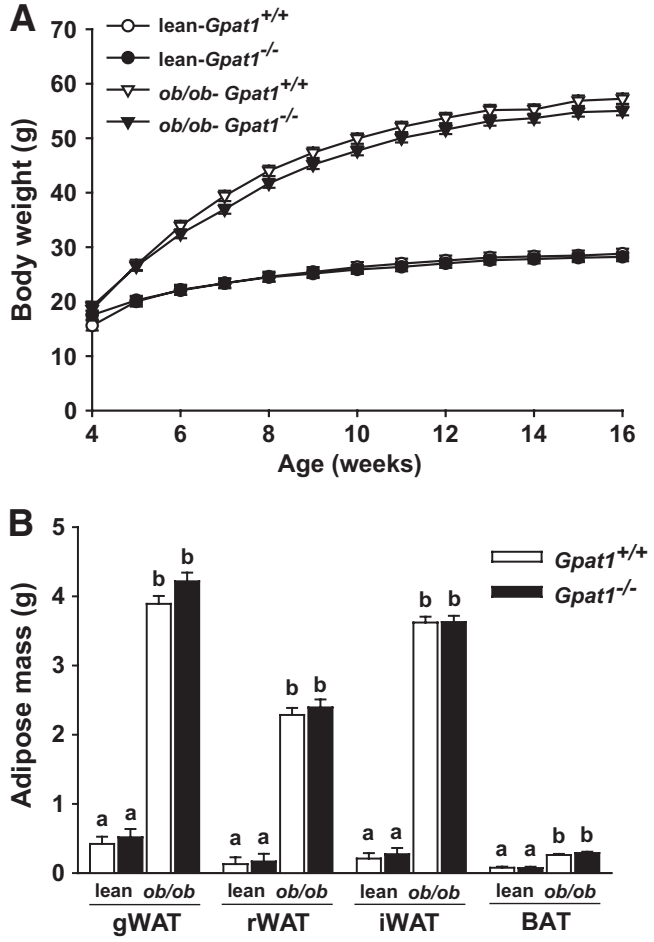

FIG. 5. *Gpat1*$^{-/-}$ mice were not resistant to genetic-induced obesity. *A*: Weight gain of lean and *ob/ob* male mice from 4 to 16 weeks of age (n = 12–17). *B*: Adipose depot weights of lean and *ob/ob* male mice at 16 weeks of age (n = 10–13). Gonadal white adipose tissue (gWAT), retroperitoneal (rWAT), inguinal (iWAT), and subscapular brown adipose tissue (BAT) depots were measured. Lean (*Lep*$^{+/?}$) and *ob/ob* (*Lep*$^{ob/ob}$). Data are LSM ± SE. Significant differences (P < 0.05) are denoted by different letters.

however, did not diminish serum lipids in *ob/ob* mice (Table 1). As reported previously in *Gpat1*$^{-/-}$ mice (16), β-hydroxybutyrate was higher in both lean and *ob/ob-Gpat1*$^{-/-}$ mice, although this effect was not statistically significant.

DISCUSSION

Several studies have demonstrated that reducing hepatic TAG content decreases hepatic insulin resistance (9,11–14). In the liver, loss- and gain-of-function studies with *Gpat1* support a role for hepatic steatosis in the development of insulin resistance (4). *Gpat1*$^{-/-}$ mice are protected from high-fat diet–induced hepatic steatosis and insulin resistance (11), whereas rats that overexpress *Gpat1* in liver have increased hepatic TAG accumulation and hepatic insulin resistance (10). Here, we show that the absence of *Gpat1* in both 6- and 16-week-old *ob/ob* mice prevents severe hepatic steatosis but does not protect against obesity-associated insulin resistance and impaired hepatic insulin signaling.

The absence of *Gpat1* reduced hepatic TAG content by 59% in *ob/ob* mice; however, the TAG content was still nearly double that of livers from lean, insulin-sensitive mice. Similarly, in *ob/ob-Srebp1*$^{-/-}$ mice, the hepatic TAG content is less than half that of *ob/ob* mice, but still almost twice that of lean mice (2). The reduced hepatic TAG content in *ob/ob-Srebp1*$^{-/-}$ mice occurs simultaneously with a 70% reduction of mRNA for hepatic *Gpat1*, a direct target of SREBP1 (5). Like our *ob/ob-Gpat1*$^{-/-}$ mice, despite marked decreases in hepatic steatosis, *ob/ob-Srebp1*$^{-/-}$ mice also remain obese and insulin resistant. In *ob/ob* mice, the absence of either *Srebp1* or *Gpat1* results in similar decreases in hepatic TAG. Thus, GPAT1 appears to be responsible for most of SREBP1-regulated hepatic TAG accumulation.

Although the hepatic TAG content of 16-week-old *ob/ob-Gpat1*$^{-/-}$ mice was similar to levels present in mice with diet-induced insulin resistance (16,34,35), even at 6 weeks, *ob/ob-Gpat1*$^{-/-}$ mice were hyperinsulinemic, insulin resistant, and had impaired hepatic insulin signaling despite the fact that their hepatic TAG content was lower than that of their insulin-sensitive lean littermates. These results demonstrate that in *ob/ob* mice, preventing hepatic steatosis did not protect against insulin resistance, which is consistent with other studies reporting a dissociation between hepatic steatosis and insulin resistance (2,16,36–38).

Because cellular TAG is stored in lipid droplets, and thus segregated from signaling events, it is believed that other, perhaps related, lipid metabolites interfere with insulin signaling pathways (15,39). Although the accumulation of acyl-CoAs has been associated with insulin resistance (40,41), mice that overexpress diacylglycerol acyltransferase-2 in liver and high-fat–fed *Gpat1*$^{-/-}$ mice have increased hepatic acyl-CoA content but do not develop insulin resistance (11,36). Hepatic acyl-CoA content is normal in *ob/ob* mice and increases when *Gpat1* is absent, but the extent of insulin resistance does not change. Thus, in *ob/ob* liver, increased acyl-CoA content itself does not impair insulin signaling. Similarly, the absence of GPAT1 increases the content of palmitoyl-CoA, the substrate for the first step in ceramide biosynthesis. However, the absence of *Gpat1* did not increase hepatic ceramide content; thus, ceramide did not contribute to hepatic insulin resistance in this model.

DAG has been most strongly associated with insulin resistance because it activates PKC-θ in the muscle (39,42) and PKC-ε in the liver (32,43), leading to reductions in downstream insulin signaling. *Gpat1*$^{-/-}$ mice that are protected from safflower oil–induced hepatic insulin resistance have reduced hepatic DAG content and PKCε activation, concomitant with improved hepatic insulin signaling (11); conversely, rats that overexpress GPAT1 in the liver show elevated DAG and PKCε activation coupled with hepatic insulin resistance (10). In the current study, however, despite normalized hepatic DAG content in *ob/ob-Gpat1*$^{-/-}$ mice, hepatic insulin signaling remained impaired. In this study, the decrease in DAG probably reflects a reduction in lipid droplet DAG content rather than membrane DAG (44), because activated PKCε was unaffected. Alternatively, a signal other than DAG that is generated during metabolic dysfunction may be responsible for PKC activation.

Studies linking reduced hepatic steatosis to improved insulin sensitivity also report concomitant decreases in adiposity (14,45). Because adipose mass was not diminished in the *ob/ob-Gpat1*$^{-/-}$ mice, any improvements in either hepatic or whole-body insulin resistance due to lower hepatic lipids could well be overshadowed by other

factors that interfere with hepatic insulin signaling (46). Rodents deficient in leptin or the leptin receptor secrete excess corticosterone (47,48). Administering a liver-selective glucocorticoid receptor antagonist to leptin receptor–deficient rats increases glucose disposal and decreases hepatic glucose production and fasting glucose (49), demonstrating that increased glucocorticoid signaling impairs hepatic and peripheral insulin sensitivity. Thus, it is likely that elevated plasma glucocorticoid levels or other obesity-related factors may have prevailed over any improvements in insulin sensitivity arising from an improved hepatic lipid profile in this model.

Fasting serum glucose and insulin concentrations were 21 and 48% higher, respectively, in *ob/ob-Gpat1*$^{-/-}$ mice than in *ob/ob* mice despite similar insulin sensitivity. Similarly, *Gpat1*$^{-/-}$ mice fed a high-fat/high-sucrose diet are less glucose tolerant and have 11% higher fasting glucose and 64% higher insulin levels than wild-type mice (16), and *ob/ob* mice with a liver-specific *Gpat1* knockdown have a twofold increase in plasma insulin (19). Hyperinsulinemia can be caused by β-cell hypertrophy and hyperplasia (50), but we did not observe differences in islet size or number (data not shown). Even at 6 weeks, lean and *ob/ob-Gpat1*$^{-/-}$ mice had 56 and 27% higher fasting insulin levels, respectively, than their *Gpat1*$^{+/+}$ counterparts (supplementary Fig. 3C), suggesting that *Gpat1*$^{-/-}$ mice are hyperinsulinemic, unrelated to the presence of insulin resistance.

In summary, we have demonstrated that GPAT1 is critical for the accumulation of TAG and DAG during the development of hepatic steatosis and is a major enzyme responsible for the lipogenic effect of SREBP1 in *ob/ob* mice (2). These results suggest that decreasing hepatic steatosis alone does not improve insulin resistance in this genetically obese model, and that factors other than increased hepatic DAG and TAG contribute to hepatic insulin resistance in *ob/ob* mice.

ACKNOWLEDGMENTS

This work was supported by National Institutes of Health (NIH) grants DK-056598 (R.A.C.), DK-40936, U24 DK-59635, and P30 DK-34987 (G.I.S.); postdoctoral fellowships from the NIH (DK-007129; A.A.W.) and the American Heart Association-Mid-Atlantic Region (L.O.L.); and an NIH grant to the UNC Clinical Nutrition Research Unit (P30 DK-56350).

No potential conflicts of interest relevant to this article were reported.

We thank Shuli Wang and Jucheng Gong for expert technical assistance.

REFERENCES

1. Zhang Y, Proenca R, Maffei M, Barone M, Leopold L, Friedman JM: Positional cloning of the mouse obese gene and its human homologue. Nature 1994;372:425–432
2. Yahagi N, Shimano H, Hasty AH, Matsuzaka T, Ide T, Yoshikawa T, Amemiya-Kudo M, Tomita S, Okazaki H, Tamura Y, Iizuka Y, Ohashi K, Osuga J, Harada K, Gotoda T, Nagai R, Ishibashi S, Yamada N. Absence of sterol regulatory element-binding protein-1 (SREBP-1) ameliorates fatty livers but not obesity or insulin resistance in Lep(ob)/Lep(ob) mice. J Biol Chem 2002;277:19353–19357
3. Gonzalez-Baró MR, Lewin TM, Coleman RA. Regulation of triglyceride metabolism: II, function of mitochondrial GPAT1 in the regulation of triacylglycerol biosynthesis and insulin action. Am J Physiol Gastrointest Liver Physiol 2007;292:G1195–G1199
4. Wendel AA, Lewin TM, Coleman RA. Glycerol-3-phosphate acyltransferases: rate limiting enzymes of triacylglycerol biosynthesis. Biochim Biophys Acta 2009;1791:501–506
5. Coleman RA, Lee DP. Enzymes of triacylglycerol synthesis and their regulation. Prog Lipid Res 2004;43:134–176
6. Shin DH, Paulauskis JD, Moustaid N, Sul HS. Transcriptional regulation of p90 with sequence homology to Escherichia coli glycerol-3-phosphate acyltransferase. J Biol Chem 1991;266:23834–23839
7. Kim HJ, Kim HJ, Lee KE, Kim DJ, Kim SK, Ahn CW, Lim SK, Kim KR, Lee HC, Huh KB, Cha BS. Metabolic significance of nonalcoholic fatty liver disease in nonobese, nondiabetic adults. Arch Intern Med 2004;164:2169–2175
8. Seppälä-Lindroos A, Vehkavaara S, Häkkinen AM, Goto T, Westerbacka J, Sovijärvi A, Halavaara J, Yki-Järvinen H. Fat accumulation in the liver is associated with defects in insulin suppression of glucose production and serum free fatty acids independent of obesity in normal men. J Clin Endocrinol Metab 2002;87:3023–3028
9. Petersen KF, Dufour S, Befroy D, Lehrke M, Hendler RE, Shulman GI. Reversal of nonalcoholic hepatic steatosis, hepatic insulin resistance, and hyperglycemia by moderate weight reduction in patients with type 2 diabetes. Diabetes 2005;54:603–608
10. Nagle CA, An J, Shiota M, Torres TP, Cline GW, Liu ZX, Wang S, Catlin RL, Shulman GI, Newgard CB, Coleman RA. Hepatic overexpression of glycerol-sn-3-phosphate acyltransferase 1 in rats causes insulin resistance. J Biol Chem 2007;282:14807–14815
11. Neschen S, Morino K, Hammond LE, Zhang D, Liu ZX, Romanelli AJ, Cline GW, Pongratz RL, Zhang XM, Choi CS, Coleman RA, Shulman GI. Prevention of hepatic steatosis and hepatic insulin resistance in mitochondrial acyl-CoA:glycerol-sn-3-phosphate acyltransferase 1 knockout mice. Cell Metab 2005;2:55–65
12. Savage DB, Choi CS, Samuel VT, Liu ZX, Zhang D, Wang A, Zhang XM, Cline GW, Yu XX, Geisler JG, Bhanot S, Monia BP, Shulman GI. Reversal of diet-induced hepatic steatosis and hepatic insulin resistance by antisense oligonucleotide inhibitors of acetyl-CoA carboxylases 1 and 2. J Clin Invest 2006;116:817–824
13. Dentin R, Benhamed F, Hainault I, Fauveau V, Foufelle F, Dyck JR, Girard J, Postic C. Liver-specific inhibition of ChREBP improves hepatic steatosis and insulin resistance in ob/ob mice. Diabetes 2006;55:2159–2170
14. Choi CS, Savage DB, Kulkarni A, Yu XX, Liu ZX, Morino K, Kim S, Distefano A, Samuel VT, Neschen S, Zhang D, Wang A, Zhang XM, Kahn M, Cline GW, Pandey SK, Geisler JG, Bhanot S, Monia BP, Shulman GI. Suppression of diacylglycerol acyltransferase-2 (DGAT2), but not DGAT1, with antisense oligonucleotides reverses diet-induced hepatic steatosis and insulin resistance. J Biol Chem 2007;282:22678–22688
15. Savage DB, Petersen KF, Shulman GI. Disordered lipid metabolism and the pathogenesis of insulin resistance. Physiol Rev 2007;87:507–520
16. Hammond LE, Neschen S, Romanelli AJ, Cline GW, Ilkayeva OR, Shulman GI, Muoio DM, Coleman RA. Mitochondrial glycerol-3-phosphate acyltransferase-1 is essential in liver for the metabolism of excess acyl-CoAs. J Biol Chem 2005;280:25629–25636
17. Yazdi M, Ahnmark A, William-Olsson L, Snaith M, Turner N, Osla F, Wedin M, Asztély AK, Elmgren A, Bohlooly-Y M, Schreyer S, Lindén D. The role of mitochondrial glycerol-3-phosphate acyltransferase-1 in regulating lipid and glucose homeostasis in high-fat diet fed mice. Biochem Biophys Res Commun 2008;369:1065–1070
18. Lindén D, William-Olsson L, Rhedin M, Asztély AK, Clapham JC, Schreyer S. Overexpression of mitochondrial GPAT in rat hepatocytes leads to decreased fatty acid oxidation and increased glycerolipid biosynthesis. J Lipid Res 2004;45:1279–1288
19. Xu H, Wilcox D, Nguyen P, Voorbach M, Suhar T, Morgan SJ, An WF, Ge L, Green J, Wu Z, Gimeno RE, Reilly R, Jacobson PB, Collins CA, Landschulz K, Surowy T. Hepatic knockdown of mitochondrial GPAT1 in ob/ob mice improves metabolic profile. Biochem Biophys Res Commun 2006;349:439–448
20. Hammond LE, Gallagher PA, Wang S, Hiller S, Kluckman KD, Posey-Marcos EL, Maeda N, Coleman RA. Mitochondrial glycerol-3-phosphate acyltransferase-deficient mice have reduced weight and liver triacylglycerol content and altered glycerolipid fatty acid composition. Mol Cell Biol 2002;22:8204–8214
21. Livak KJ, Schmittgen TD. Analysis of relative gene expression data using real-time quantitative PCR and the 2(-Delta Delta C(T)) method. Methods 2001;25:402–408
22. Folch J, Lees M, Sloane Stanley GH. A simple method for the isolation and purification of total lipides from animal tissues. J Biol Chem 1957;226:497–509
23. Danno H, Jincho Y, Budiyanto S, Furukawa Y, Kimura S. A simple enzymatic quantitative analysis of triglycerides in tissues. J Nutr Sci Vitaminol (Tokyo) 1992;38:517–521

24. Wolever TM, Jenkins DJ, Jenkins AL, Josse RG: The glycemic index: methodology and clinical implications. Am J Clin Nutr 1991;54:846–854
25. Qu X, Seale JP, Donnelly R. Tissue and isoform-selective activation of protein kinase C in insulin-resistant obese Zucker rats: effects of feeding. J Endocrinol 1999;162:207–214
26. Donnelly R, Reed MJ, Azhar S, Reaven GM. Expression of the major isoenzyme of protein kinase-C in skeletal muscle, nPKC theta, varies with muscle type and in response to fructose-induced insulin resistance. Endocrinology 1994;135:2369–2374
27. Shimomura I, Bashmakov Y, Horton JD. Increased levels of nuclear SREBP-1c associated with fatty livers in two mouse models of diabetes mellitus. J Biol Chem 1999;274:30028–30032
28. Mayer J, Bates MW, Dickie MM. Hereditary diabetes in genetically obese mice. Science 1951;113:746–747
29. Shulman GI. Cellular mechanisms of insulin resistance. J Clin Invest 2000;106:171–176
30. Nagle CA, Klett EL, Coleman RA. Hepatic triacylglycerol accumulation and insulin resistance. J Lipid Res 2009;50(Suppl.):S74–S79
31. Holland WL, Brozinick JT, Wang LP, Hawkins ED, Sargent KM, Liu Y, Narra K, Hoehn KL, Knotts TA, Siesky A, Nelson DH, Karathanasis SK, Fontenot GK, Birnbaum MJ, Summers SA. Inhibition of ceramide synthesis ameliorates glucocorticoid-, saturated-fat-, and obesity-induced insulin resistance. Cell Metab 2007;5:167–179
32. Samuel VT, Liu ZX, Wang A, Beddow SA, Geisler JG, Kahn M, Zhang XM, Monia BP, Bhanot S, Shulman GI. Inhibition of protein kinase Cepsilon prevents hepatic insulin resistance in nonalcoholic fatty liver disease. J Clin Invest 2007;117:739–745
33. Lindström P. The physiology of obese-hyperglycemic mice [ob/ob mice]. ScientificWorldJournal 2007;7:666–685
34. Yu XX, Murray SF, Pandey SK, Booten SL, Bao D, Song XZ, Kelly S, Chen S, McKay R, Monia BP, Bhanot S. Antisense oligonucleotide reduction of DGAT2 expression improves hepatic steatosis and hyperlipidemia in obese mice. Hepatology 2005;42:362–371
35. Morgan K, Uyuni A, Nandgiri G, Mao L, Castaneda L, Kathirvel E, French SW, Morgan TR. Altered expression of transcription factors and genes regulating lipogenesis in liver and adipose tissue of mice with high fat diet-induced obesity and nonalcoholic fatty liver disease. Eur J Gastroenterol Hepatol 2008;20:843–854
36. Monetti M, Levin MC, Watt MJ, Sajan MP, Marmor S, Hubbard BK, Stevens RD, Bain JR, Newgard CB, Farese RV Sr, Hevener AL, Farese RV Jr. Dissociation of hepatic steatosis and insulin resistance in mice overexpressing DGAT in the liver. Cell Metab 2007;6:69–78
37. Matsuzaka T, Shimano H, Yahagi N, Kato T, Atsumi A, Yamamoto T, Inoue N, Ishikawa M, Okada S, Ishigaki N, Iwasaki H, Iwasaki Y, Karasawa T, Kumadaki S, Matsui T, Sekiya M, Ohashi K, Hasty AH, Nakagawa Y, Takahashi A, Suzuki H, Yatoh S, Sone H, Toyoshima H, Osuga J, Yamada N. Crucial role of a long-chain fatty acid elongase, Elovl6, in obesity-induced insulin resistance. Nat Med 2007;13:1193–1202
38. Grefhorst A, Hoekstra J, Derks TG, Ouwens DM, Baller JF, Havinga R, Havekes LM, Romijn JA, Kuipers F. Acute hepatic steatosis in mice by blocking beta-oxidation does not reduce insulin sensitivity of very-low-density lipoprotein production. Am J Physiol Gastrointest Liver Physiol 2005;289:G592–G598
39. Yu C, Chen Y, Cline GW, Zhang D, Zong H, Wang Y, Bergeron R, Kim JK, Cushman SW, Cooney GJ, Atcheson B, White MF, Kraegen EW, Shulman GI. Mechanism by which fatty acids inhibit insulin activation of insulin receptor substrate-1 (IRS-1)-associated phosphatidylinositol 3-kinase activity in muscle. J Biol Chem 2002;277:50230–50236
40. Kim JK, Fillmore JJ, Chen Y, Yu C, Moore IK, Pypaert M, Lutz EP, Kako Y, Velez-Carrasco W, Goldberg IJ, Breslow JL, Shulman GI. Tissue-specific overexpression of lipoprotein lipase causes tissue-specific insulin resistance. Proc Natl Acad Sci U S A 2001;98:7522–7527
41. Kim JK, Gimeno RE, Higashimori T, Kim HJ, Choi H, Punreddy S, Mozell RL, Tan G, Stricker-Krongrad A, Hirsch DJ, Fillmore JJ, Liu ZX, Dong J, Cline G, Stahl A, Lodish HF, Shulman GI. Inactivation of fatty acid transport protein 1 prevents fat-induced insulin resistance in skeletal muscle. J Clin Invest 2004;113:756–763
42. Griffin ME, Marcucci MJ, Cline GW, Bell K, Barucci N, Lee D, Goodyear LJ, Kraegen EW, White MF, Shulman GI. Free fatty acid-induced insulin resistance is associated with activation of protein kinase C theta and alterations in the insulin signaling cascade. Diabetes 1999;48:1270–1274
43. Samuel VT, Liu ZX, Qu X, Elder BD, Bilz S, Befroy D, Romanelli AJ, Shulman GI. Mechanism of hepatic insulin resistance in non-alcoholic fatty liver disease. J Biol Chem 2004;279:32345–32353
44. Shin OH, da Costa KA, Mar MH, Zeisel SH. Hepatic protein kinase C is not activated despite high intracellular 1,2-sn-diacylglycerol in obese Zucker rats. Biochim Biophys Acta 1997;1358:72–78
45. Ntambi JM, Miyazaki M, Stoehr JP, Lan H, Kendziorski CM, Yandell BS, Song Y, Cohen P, Friedman JM, Attie AD. Loss of stearoyl-CoA desaturase-1 function protects mice against adiposity. Proc Natl Acad Sci U S A 2002;99:11482–11486
46. Kahn BB, Flier JS. Obesity and insulin resistance. J Clin Invest 2000;106:473–481
47. Livingstone DE, Jones GC, Smith K, Jamieson PM, Andrew R, Kenyon CJ, Walker BR. Understanding the role of glucocorticoids in obesity: tissue-specific alterations of corticosterone metabolism in obese Zucker rats. Endocrinology 2000;141:560–563
48. Livingstone DE, Grassick SL, Currie GL, Walker BR, Andrew R. Dysregulation of glucocorticoid metabolism in murine obesity: comparable effects of leptin resistance and deficiency. J Endocrinol 2009;201:211–218
49. Zinker B, Mika A, Nguyen P, Wilcox D, Ohman L, von Geldern TW, Opgenorth T, Jacobson P. Liver-selective glucocorticoid receptor antagonism decreases glucose production and increases glucose disposal, ameliorating insulin resistance. Metabolism 2007;56:380–387
50. Summers SA, Nelson DH. A role for sphingolipids in producing the common features of type 2 diabetes, metabolic syndrome X, and Cushing's syndrome. Diabetes 2005;54:591–602